

# Attributes and influence on fluid flow of fractures in foreland carbonates of southern Italy

Andrea Billi\*

*Dipartimento di Scienze Geologiche, Università Roma Tre, Largo S.L. Murialdo 1, 00146 Rome, Italy*

Received 17 September 2004; received in revised form 1 May 2005; accepted 9 May 2005

Available online 7 July 2005

## Abstract

The geometrical and structural attributes of fractures and fracture networks affecting Mesozoic–Cenozoic, platform carbonates from foreland areas of southern Italy are qualitatively and quantitatively described. Fractures include faults, joints and fault-related solution cleavages. Two tectonic environments can be recognised: (1) the Apulian and Hyblean forebulge domains, consisting of broad foreland areas, where joints and rare, low-displacement, normal faults occur and (2) the Gargano strike-slip fault domain, where strike-slip faults and fault-related solution cleavages are the most ubiquitous structures. In both tectonic environments, orthogonal sets of sub-vertical fractures separate the beds into an assemblage of fracture-bound blocks commonly characterised by an orthorhombic symmetry and a centimetric-to-metric size. The general causes for the observed fractures are ascribed to the bending stress in the Apulian and Hyblean forebulge domains and to the strike-slip faulting in the Gargano area. Fracture attributes and distributions suggest that the rock permeability is markedly anisotropic in both tectonic environments.

© 2005 Elsevier Ltd. All rights reserved.

*Keywords:* Flexure; Fluid flow; Foreland; Fracture; Joint; Solution cleavage

## 1. Introduction

The influence that fractures exert on fluid flow through rocks (e.g. Engelder and Scholz, 1981; Sibson, 1996; Eichubl et al., 2004) makes genetic and structural studies of fracturing relevant to geologists from different fields of study. Fracture networks can control the infiltration and percolation of groundwater or chemical and radioactive contaminants (e.g. Brusseau, 1994; Caine and Tomusiak, 2003), the migration and accumulation of hydrocarbons (e.g. Narr and Currie, 1982; Dholakia et al., 1998), the circulation of geothermal fluids (e.g. Gudmundsson, 2000) and the distribution of economically relevant mineralisations (e.g. Blenkinsop et al., 2004).

Computer modelling has recently improved the understanding of rock fracture-related permeability (e.g. de Dreuzy et al., 2001; Darcel et al., 2004), but knowledge of

the in situ structural and geometrical attributes of fractures and fracture networks is still fundamental if the proper data are to be input into models of fluid flow and transport simulators (e.g. Taylor et al., 1999; Gerritsen and Durlofsky, 2005). It is known that fluid flow in fractured rocks of very low matrix permeability is usually characterised by scale dependence and by marked anisotropy (Neretnieks, 1985; Neuman and Di Federico, 2003). This is demonstrated by the disparate permeability of fractured rocks at laboratory to borehole scales (Clauser, 1992) and by the different amounts of flow through vertical and properly deviated boreholes drilled in the same hydrocarbon reservoir (e.g. Nelson, 2001). The anisotropy and scale dependence of rock permeability are connected with the heterogeneous structural and geometrical attributes of fractures (e.g. Odling et al., 1999). Despite a vast literature on rock fractures, their structural and geometrical attributes in foreland areas are still poorly known because of the common misconception of a substantial absence of deformations in these areas. Yet foreland fractured rocks are known to carry important aquifers and hydrocarbon reservoirs (e.g. Mattavelli et al., 1993).

The principal aim of this paper is to provide the

\* Tel.: +39 06548 88016; fax: +39 06548 88201.

E-mail address: billi@uniroma3.it.

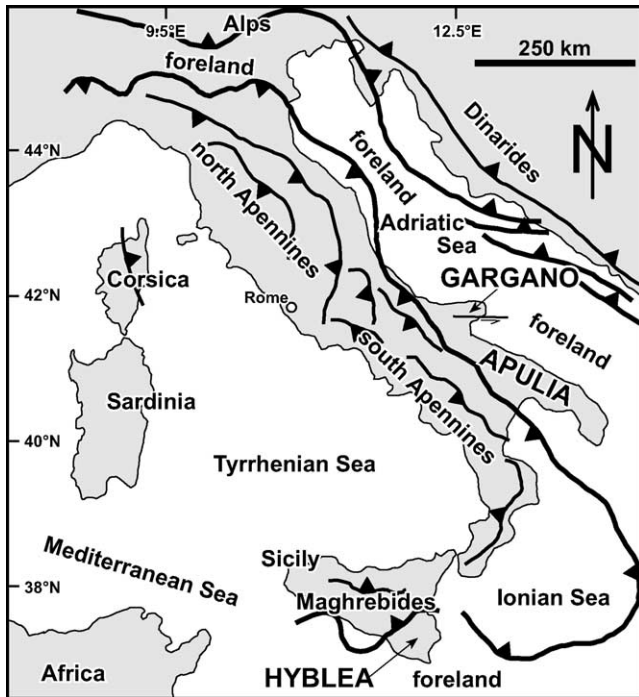


Fig. 1. Map of Italy and surrounding regions with major thrust fronts. Note the Apulian, Hyblean, and Gargano study areas located in foreland regions.

geometrical and structural characterisation of fractured carbonate beds observed in exposures of two foreland areas in southern Italy, namely the Apulian and Hyblean forelands (Fig. 1). Attributes of fractures and fracture networks from vast foreland regions are qualitatively and quantitatively presented. The general causes for the observed fractures are discussed. Inferences for the hydraulic properties of foreland carbonate beds at shallow depths are addressed.

## 2. Geological setting

The Apulian and Hyblean plateaus are onshore, continental, foreland regions along the Apenninic–Maghrebic fold–thrust belt (Fig. 1). This contractional belt developed during Cenozoic by the convergence between the African and Eurasian plates in the central Mediterranean (Dewey et al., 1989). The progressive time–space migration of the fold–thrust belt occurred simultaneously with the flexural retreat (or roll-back) of the foreland lithosphere toward the east and the south (Malinverno and Ryan, 1986). Different amounts and rates of flexural retreats in adjacent foreland compartments generated non-cylindrical flexure, foreland segmentation, and transverse accommodation faults (Royden et al., 1987; Favali et al., 1993; Mariotti and Doglioni, 2000).

The Apulian Plateau in southeastern Italy (Fig. 2) forms the modern forebulge of the flexed Adriatic foreland. The NW-trending (i.e. hinge trend) forebulge formed by flexure

of the continental Adriatic lithosphere, mostly during Pliocene–Pleistocene (Royden et al., 1987; Patacca and Scandone, 2001). The Apulian Plateau consists of Mesozoic platform carbonates more than 6 km thick occurring over a Variscan crystalline basement (D’Argenio, 1974). The exposed rocks are mostly carbonates of Cretaceous and Jurassic age. Although in the Apulian Plateau area (Fig. 2a) the forebulge has a near-cylindrical shape, its overall geometry at the regional scale is markedly non-cylindrical (Royden et al., 1987; Mariotti and Doglioni, 2000; Bertotti et al., 2001). Toward the northwest and the southeast, where the forebulge laterally fades, the NW-trending flexure hinge slightly plunges toward the northwest and the southeast, respectively, thus revealing a slight, doubly-plunging shape of the Apulian forebulge (i.e. NE–SW as the major plunging direction and NW–SE as the secondary one). Toward the northeast and the southwest, the forebulge is bounded by NW-striking normal faults (Fig. 2).

The Gargano Peninsula is located to the northwest of the Apulian Plateau (Fig. 2). In the Gargano area, a transcontractional belt associated with the left-lateral, strike-slip Mattinata Fault (Salvini et al., 1999; Brankman and Aydin, 2004) transversally dissects the Apulian forebulge. The formation of this strike-slip fault belt is probably related to the differential flexural retreats in the adjacent foreland compartments (Favali et al., 1993; Doglioni et al., 1994). The Gargano strike-slip belt formed since the Pliocene at least and is still active, as demonstrated by its seismic activity (Favali et al., 1993).

The Hyblean Plateau in southeastern Sicily (Fig. 3) forms the modern forebulge of the continental Pelagian foreland (Cogan et al., 1989; Barrier, 1992), which is the northern edge of the African foreland. The Hyblean Plateau consists of a thick, Mesozoic–Cenozoic sequence of carbonate rocks underlain by a continental basement of unknown age. The thickness of the sedimentary cover in the Hyblean Plateau is ~6 km (Zarudski, 1972; Yellin-Dror et al., 1997). The Hyblean forebulge is a non-cylindrical structure (Ben-Avraham et al., 1995), with a major NW–SE plunging direction and a subordinate NE–SW one. Such a doubly-plunging structure formed by a complex flexure of the continental lithosphere since at least the mid-Miocene and probably until the Pleistocene (Grasso and Pedley, 1990). The double plunging shape of the Hyblean foreland is due to the development of two orogenic salients (i.e. forelandward convex arcs) that partly surrounded the Hyblean forebulge (Fig. 1). The load of the orogenic salients on the northeastern and southwestern sides of the Hyblean region caused its plunging also toward the northeast and the southwest.

## 3. Key terms

Definitions or specifications for some key terms used in this paper are as follows:

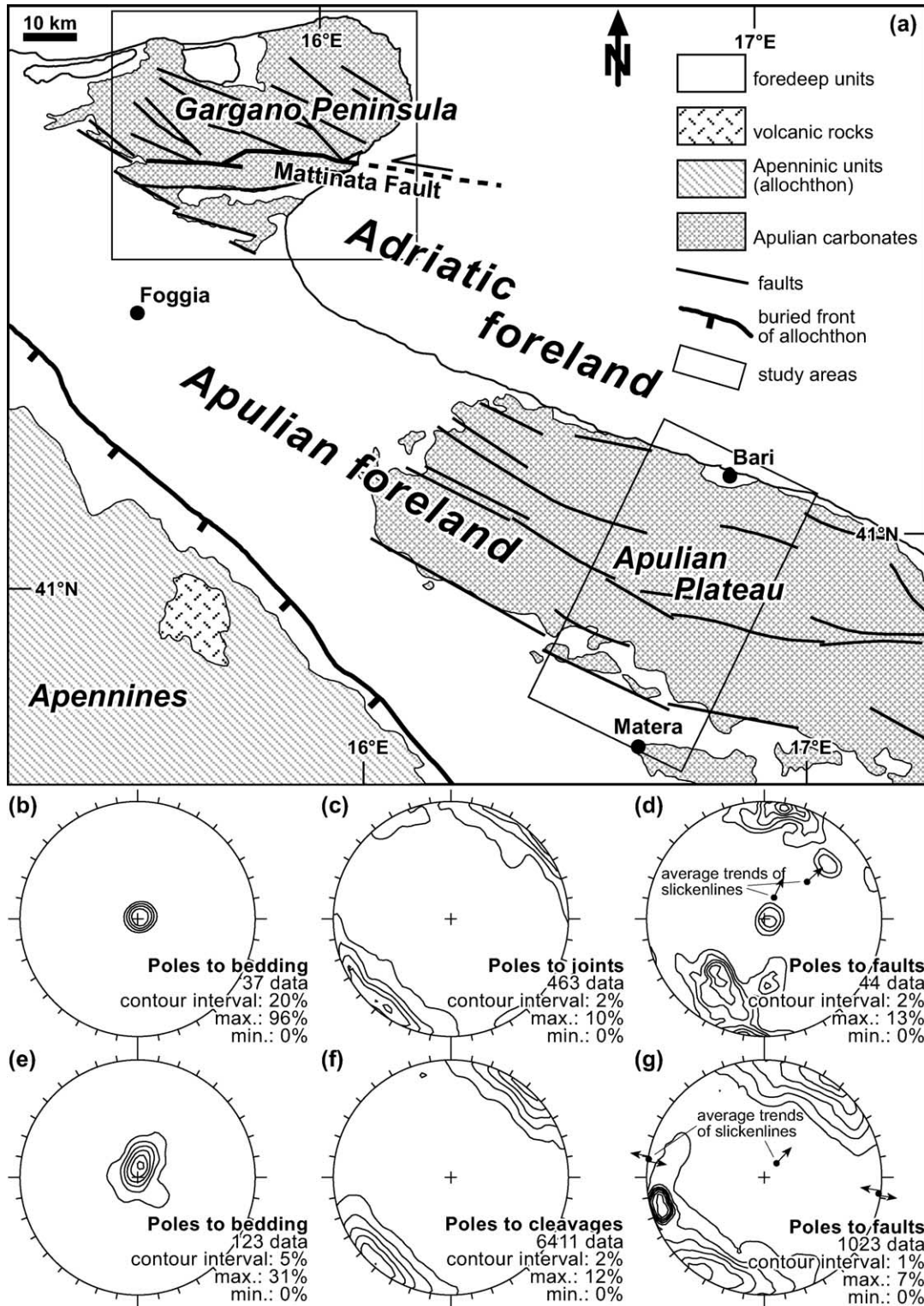


Fig. 2. (a) Map of the Apulian foreland. Rectangular insets indicate the study areas (i.e. the Apulian Plateau and the Gargano Peninsula). (b)–(d) Schimdt nets (lower hemisphere) of structural data collected over the Apulian Plateau (forebulge domain) in sites located away (> 200 m) from major faults. (e)–(g) Schimdt nets (lower hemisphere) of structural data collected in the Gargano Peninsula along the Mattinata Fault system (strike-slip fault domain).

(1) ‘Fracture’ is used as a general term to indicate a rock structure with two facing and sub-parallel surfaces across which there has been loss of rock continuity and, therefore, strength, due to tectonics (Pollard and Aydin,

1988). In this paper, fractures include faults (tangential displacement), joints (dilatational displacement), and fault-related, solution cleavages (anti-dilatational displacement), but also structures characterised by



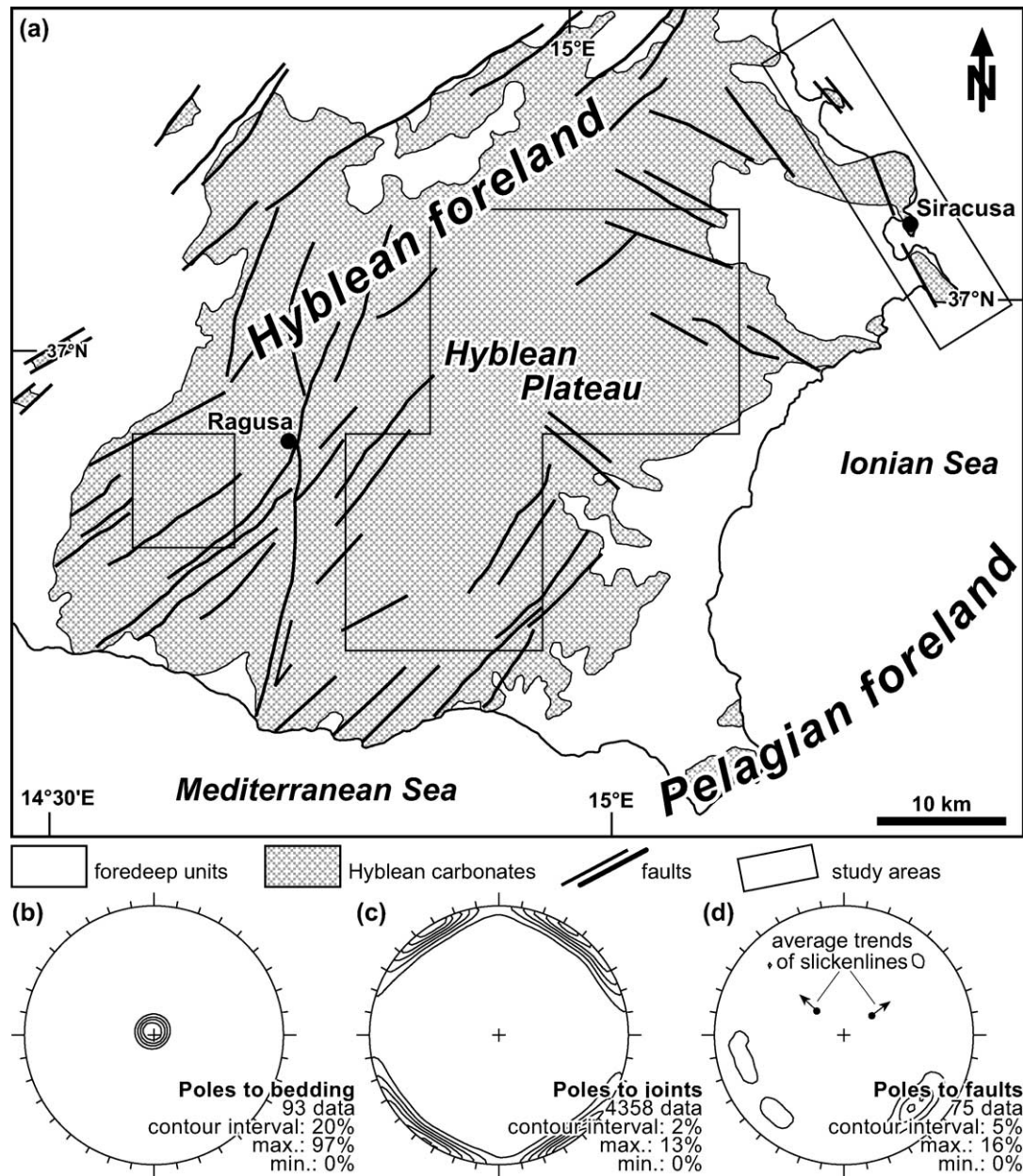


Fig. 3. (a) Map of the Hyblean foreland. Rectangular and polygonal insets indicate the study areas (i.e. the Hyblean Plateau). (b)–(d) Schimdt nets (lower hemisphere) of structural data collected over the Hyblean Plateau (forebulge domain) in sites located away (>200 m) from major faults.

complex evolutions such as solution cleavages that have post-dissolution, dilational or tangential displacements.

- (2) ‘Solution cleavage’ is used to indicate a rock discontinuity nucleated and propagated by dissolution of carbonates (i.e. anti-dilational displacement; Fletcher and Pollard, 1981) under a tectonic load, usually within a fault damage zone. In the Gargano study area, most solution cleavages show a post-dissolution dilational displacement and, occasionally, a post-dissolution tangential displacement (Salvini et al., 1999). In these cases, the term solution cleavage refers to the primary nature of these tectonic discontinuities.
- (3) ‘Bedding surface’ is used to indicate a distinct surface

separating two adjacent beds. In the study areas, the bedding surfaces constitute marked mechanical discontinuities, which halted the propagation of joints and solution cleavages.

- (4) ‘Bed-parting’ and ‘bed-unparting’ are used to indicate two types of fractures (i.e. usually perpendicular to bedding) as observed in the study areas (Fig. 4). Bed-parting fractures are those that cut a single bed entirely and separate it into distinct parts, which are hereafter called ‘fracture-bound blocks’ (Fig. 4). The trace and the displacement (i.e. usually a dilational or a tangential displacement) of these fractures are discernible both on bedding surfaces and on bed cross-sections (Fig. 4b

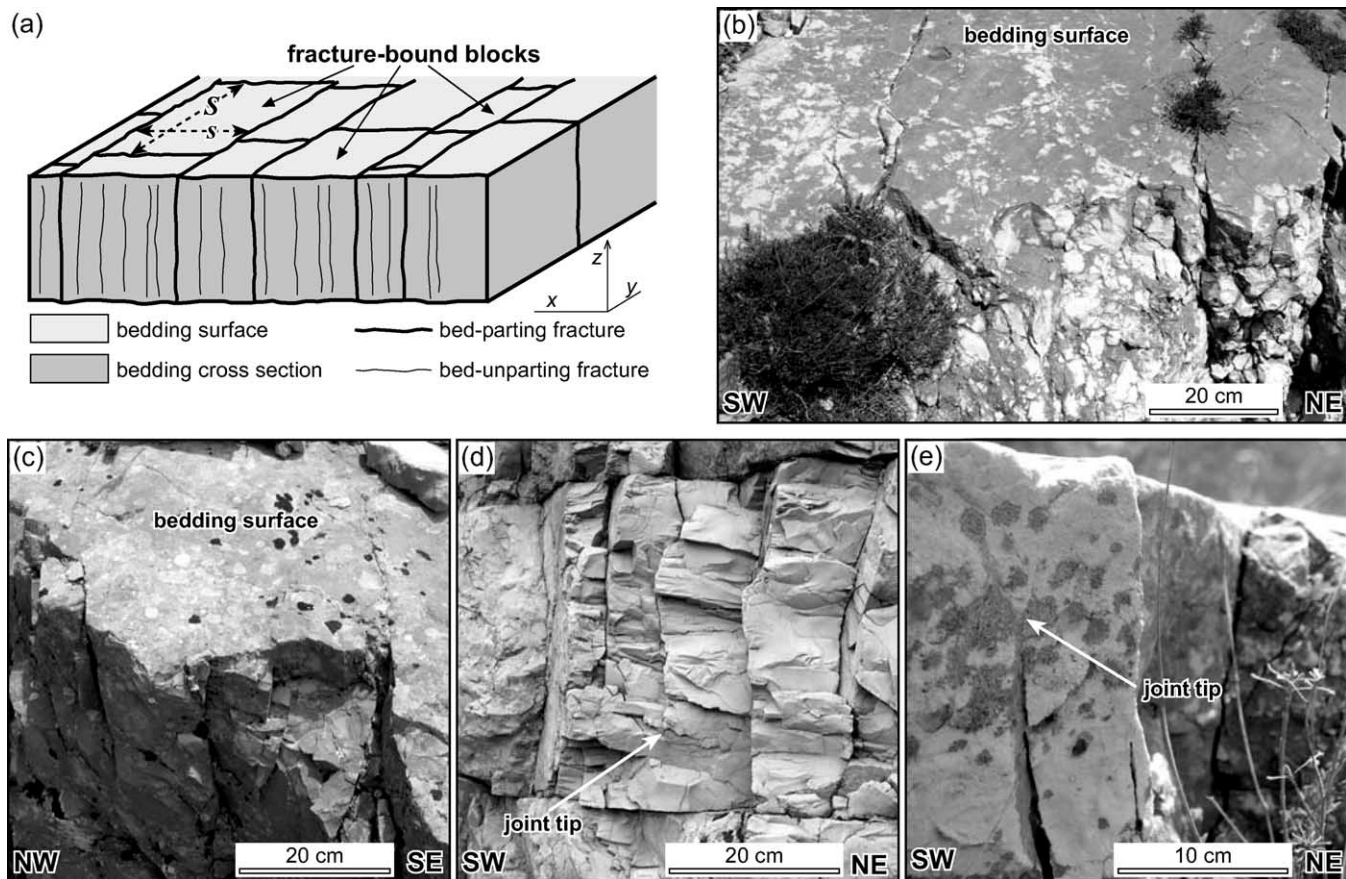


Fig. 4. (a) Block diagram illustrating an ideal carbonate bed lying horizontally and affected by orthogonal, sub-vertical fractures. Some fractures are bed-parting and some others are bed-unparting.  $S$  and  $s$  are dimensions (i.e. long and short sides, respectively) for determining the aspect ratio of fracture-bound blocks.  $S$  and  $s$  are measured over the bedding surface and are determined by intersecting, bed-parting fractures. The aspect ratio of fracture-bound blocks is the ratio between  $S$  and  $s$ . Fracture-bound blocks may contain bed-unparting fractures. (b) and (c) Photographs of fractured carbonate beds showing bed-parting (on bedding surfaces) and bed unparting (only on bed cross-sections) fractures. (b) From the Gargano Peninsula. (c) From the Hyblean Plateau. (d) Photograph (from the Apulian Plateau) showing joints within carbonate beds. One joint (indicated by the arrow) is bed-unparting. Note its tip lying within the bed. (e) Photograph (from the Apulian Plateau) showing a bed-unparting joint. Note the joint tip (indicated by the arrow) lying within the bed.

and c). Bed-unparting fractures are contained within a single bed and do not separate the bed into fracture-bound blocks (Fig. 4d and e). The trace and displacement of bed-unparting fractures cannot be discerned on bedding surfaces but only on bed cross-sections.

## 4. Results

### 4.1. Fractures in the forebulge domains

The most ubiquitous structures in the Apulian and Hyblean forebulge domains are orthogonal sets of joints affecting the Mesozoic–Cenozoic carbonate beds (Figs. 4 and 5). Plumose structures (Fig. 5a) commonly occur over the joint surfaces and show the dilational origin of these structures (e.g. Kulander and Dean, 1985; Pollard and Aydin, 1988).

In the Apulian Plateau, upper Cretaceous, shallow-water carbonates are characterised by horizontal or gently dipping beds ( $<5^\circ$ ; Fig. 2b). Bed thickness varies from 0.2 m to more than 2 m. Two major sets of sub-vertical joints affect the carbonate beds, those striking NW–SE and NE–SW, respectively (e.g. Fig. 5c). The most frequent set is the NW-striking one. The NE-striking set consists of joints shorter than the NW-striking ones. The NE-striking joints usually abut against the NW-striking ones. Most joints in the Apulian Plateau are bed-unparting structures, well discernible on vertical cross-sections of beds (Fig. 4d and e). A limited number of joints are bed-parting (Figs. 4d and 5c).

Rare, normal faults in the study sites of the Apulian Plateau are high-angle ( $\geq 60^\circ$ ), have low-displacement (throw  $<30$  cm) and strike preferentially NW–SE and WNW–ESE (Fig. 2d). These faults commonly generate limited downbending of beds (Fig. 5e). Faults have dip-slip slickenside lineations (Fig. 2d). Gouge and other strongly comminuted fault rocks are usually absent or poorly developed along faults.



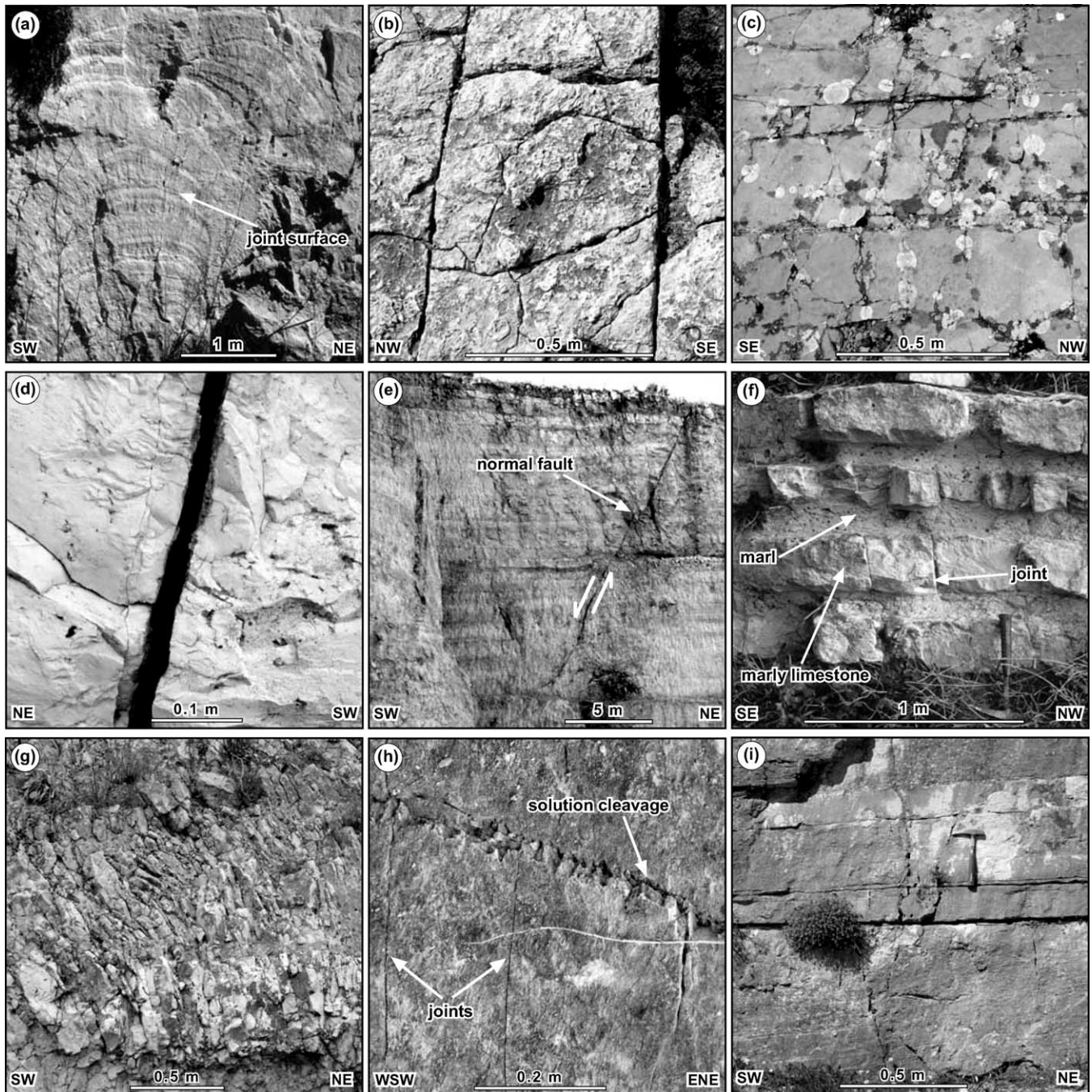


Fig. 5. Photographs of carbonate rock exposures from the Apulian and Hyblean forelands. (a) Plumose structure over a vertical joint surface (Hyblean Plateau). (b) Orthogonal joints observed over a bedding surface (map view, Hyblean Plateau). The NW-striking joints abut against the longer, NE-striking ones. (c) Orthogonal joints observed over a bedding surface (map view, Apulian Plateau). The NE-striking joints abut against the longer, NW-striking ones. (d) Detail of an open joint in a bed cross-section (Apulian Plateau). (e) Normal fault across jointed carbonate beds in the Apulian Plateau. (f) Alternating layers of soft marls and strong marly limestones (Hyblean Plateau). Joints affect only the strong marly limestone. (g) Solution cleavage across Jurassic beds in the Gargano Peninsula (cross-section view). (h) Solution cleavage with a stylolitic profile as observed over a bedding surface (map view, Gargano Peninsula). Note also the secondary joints, which abut against the cleavage surface. (i) Undeformed carbonate beds lying outside the major fault zones in the Gargano Peninsula (cross-section view).

Joints in the Hyblean Plateau occur in Miocene carbonate beds, which are horizontal or gently dipping ( $<5^\circ$ ; Fig. 3b). Beds range from 0.1 m to about 3 m thick. Massive carbonates also occur. Two major sets of sub-vertical joints

intersect at about  $90^\circ$  (Figs. 3c and 5b). In particular, an earliest set of joints strikes NE–SW, whereas a later set, consisting of shorter surfaces usually abutting against the NE-striking joints, strikes NW–SE. Similar to the joints

observed in the Apulian Plateau, most joints in the Hyblean Plateau are bed-unparting and relatively few are bed-parting (Fig. 4c). Thin beds (i.e. between 5 and 80 cm thick) of soft marls occasionally occur in the carbonate succession and are rarely affected by joints (Fig. 5f).

Rare, normal faults exposed in the study sites of the Hyblean Plateau are high-angle ( $\geq 60^\circ$ ), have low-displacement (throw  $< 10$ – $20$  cm) and strike preferentially NW–SE and NE–SW (Fig. 3d). These faults generate limited downbending of beds. Gouge and other strongly comminuted fault rocks are usually absent from or poorly developed along the fault surfaces. The normal faults have dip-slip slickenside lineations (Fig. 3d).

#### 4.2. Fractures in the Gargano strike-slip fault domain

Fractures in the Gargano Peninsula occur in Mesozoic, shallow-water carbonate beds within left-lateral, strike-slip fault zones, which are tens to hundreds of metres thick and tens of kilometres long (Fig. 2a). Beds strike WNW–ESE and dip at up to  $35^\circ$  toward the S–SW or toward the N–NE (Fig. 2e). Bed thickness is between 0.2 m and more than 2 m. Fractures are mainly NW-striking solution cleavages (Figs. 2f, 4b and 5g and h) developed within the E–W-striking Mattinata Fault and along other E–W- to NW–SE-striking strike-slip fault zones (Fig. 2a and g). Solution cleavages are sub-vertical (Fig. 2f) and are usually perpendicular to beds. Outside the fault zones, only rare and poorly systematic joints affect the carbonate beds (Fig. 5i). Cleavage surfaces are usually characterised by an anastomosing, undulating profile (Fig. 5g) and by a dilational displacement of less than 3–4 mm. Some cleavage surfaces are stylolitic (Fig. 5h). Most cleavage surfaces are bed-unparting (Fig. 4b). Bed-parting cleavages are usually those characterised by well-evident dilational or strike-slip displacement. The frequency of bed-parting cleavage increases toward the fault cores (i.e. the cleavage spacing decreases), where most of the shear displacement is accommodated (e.g. Caine et al., 1996). The sub-vertical cleavage-bounded blocks are usually affected by sub-horizontal and sub-vertical joints, which abut against the cleavage surfaces. In approaching the fault cores, these joints are progressively more frequent.

Layers of fine-grained cataclastic rocks usually occur along polished fault surfaces within the fault cores. The fault-perpendicular thickness of these cataclastic zones varies between a few centimetres and 20–30 m (e.g. Billi and Storti, 2004).

#### 4.3. Fracture spacing and aspect ratio of fracture-bound blocks

The spacing of fractures is the perpendicular distance between two adjacent and sub-parallel fracture surfaces (e.g. Price, 1966). The fracture spacing for the major set

in each study area is hereafter considered, namely the NW-trending joints in the Apulian Plateau (Fig. 2c), the NE-trending joints in the Hyblean Plateau (Fig. 3c), and the NW-trending solution cleavages in the Gargano Peninsula (Fig. 2f). Fig. 6 shows diagrams of fracture spacing versus bed thickness, as sorted by study areas and fracture types. Each fracture spacing datum on the y-axes of these diagrams is the mean value computed from a Gaussian best fitting (e.g. Salvini et al., 1999) of the population of fracture spacing from a single scan-line (i.e. a sample line across fractures in a single bed). The length of scan-lines (i.e. between 1 and 20 m) was chosen as statistically appropriate for the sampling of fracture spacing in each bed. Fig. 6 shows an overall direct relationship between fracture spacing and bed thickness, although the correlation is less evident between solution cleavage and bed thickness (Fig. 6e). For the same bed thickness, the spacing of bed-parting fractures (Fig. 6b, d and f) is between about two and five times greater than the spacing of fractures measured on the bed cross-sections (i.e. including both bed-unparting and bed-parting fractures; Fig. 6a, c and e). When measured on the bed cross-sections (i.e. bed-parting and bed-unparting fractures), the spacing of joints (Fig. 6a and c) is about twice that of solution cleavages (Fig. 6e), whereas when measured on bedding surfaces (i.e. only bed-parting fractures), the spacing of joints (Fig. 6b and d) is the same as or slightly greater than that of solution cleavages (Fig. 6f).

The two-dimensional aspect ratio of fracture-bound blocks (i.e. as observed on bedding surfaces) was determined by dividing their long side into the short side (i.e.  $S$  versus  $s$  in Fig. 4a). Fig. 7 shows diagrams of aspect ratio versus bed thickness, as sorted by study areas. Each aspect ratio datum on the y-axes of diagrams in Fig. 7 is the mean value computed from a Gaussian best fitting of the population of aspect ratios from a single scan-area (i.e. a sample area on a single bedding surface). The size of scan-areas was chosen as statistically appropriate for the sampling of the aspect ratio of fracture-bound blocks on each bed. Diagrams in Fig. 7 show a direct and approximately linear relationship between the aspect ratio and the corresponding bed thickness. This relationship applies both to the joint-bound blocks (i.e. Apulian and Hyblean plateaus; Fig. 7a and b) and to the cleavage-bound blocks (i.e. Gargano Peninsula; Fig. 7c). For the same bed thickness, the aspect ratio is about the same both for the joint-bound blocks in the Apulian and Hyblean plateaus and for the cleavage-bound blocks in the Gargano Peninsula (e.g. in Fig. 7a–c, aspect ratio  $\approx 4$  for bed thickness  $\approx 40$  cm).

#### 4.4. Fracture aperture

A wedge-shaped metal calliper with a resolution of 0.5 mm was used to measure the aperture of fractures (i.e. the maximum dilational displacement perpendicular to the fracture walls). To minimize the effect of weathering on the measurement of fracture apertures, only beds exposed on



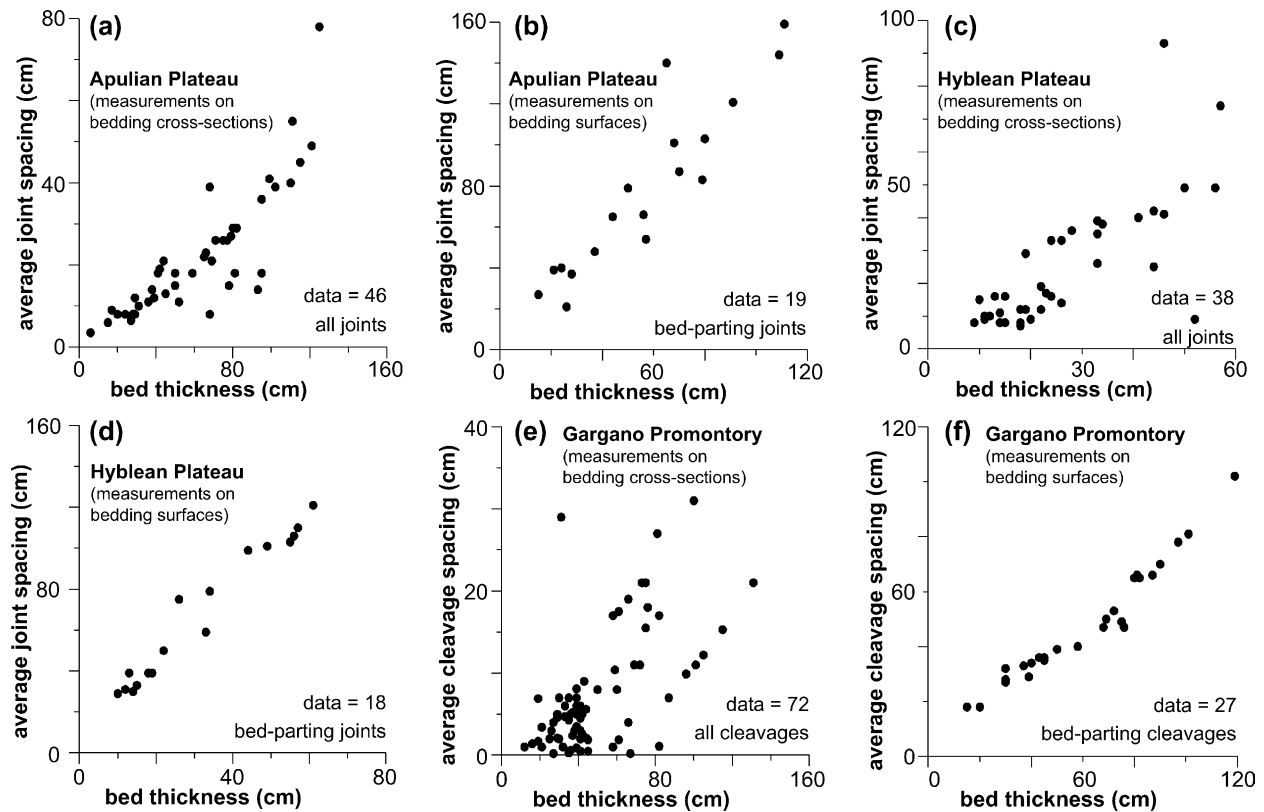


Fig. 6. Diagrams of the average joint and cleavage spacing against the thickness of beds. (a), (c) and (e) show the spacing of all fractures (i.e. bed-unparting and bed-parting), whereas (b), (d) and (f) show the spacing of only the bed-parting fractures. These diagrams show an overall direct correlation between bed thickness and fracture spacing (including bed-parting and bed-unparting joints and cleavage).

active quarry fronts or on fresh roadcuts were considered. Because the aperture of fractures usually tends to reduce from the mid-plane of beds toward their top and bottom boundary surfaces (i.e. particularly for the bed-unparting fractures), fracture apertures were measured along the mid-plane of beds, where the fracture aperture was about maximum. The true maximum aperture of fractures, however, is difficult to obtain because of the irregular geometry of fractures (e.g. Aydin, 2000). Moreover, the fracture aperture usually decreases with increasing confining pressures (i.e. increasing depths). For these reasons, the data hereafter provided should be considered as the upper bound for the fracture aperture in the study areas.

Fig. 8 shows the fracture aperture as frequency histograms of data collected along 18 selected scan-lines across different beds. The thickness of beds containing the analysed fractures ranges between 26 cm (Fig. 8a and m) and 94 cm (Fig. 8o). The aperture of the analysed fractures is between 0.5 and 35 mm (Fig. 8). In each study area, the average aperture of fractures (either joints or cleavages) is greater for thicker beds (e.g. compare Fig. 8a–c) and for the bed-parting fractures (e.g. compare Fig. 8m and p). Moreover, the aperture of joints is averagely greater (at least double for similar thicknesses of beds) than the aperture of cleavages (compare Fig. 8a–l with Fig. 8m–r).

## 5. Discussion

### 5.1. Fracture development

The general causes for the formation of the fractures observed over the studied foreland areas are hereafter considered. The causes for specific issues such as the development of bed-parting and bed-unparting fractures or the correlations between bed thickness and fracture attributes (i.e. fracture spacing, aspect ratio of fracture-bound blocks and fracture aperture in Figs. 6–8, respectively) are beyond the scope of this paper and will be the subject of a paper in preparation. Moreover, the causes for the fracture spacing in layered rocks are widely addressed in the literature (e.g. Gross, 1993; Gillespie et al., 1999; Bai et al., 2000).

Flexure of foreland lithospheres near orogenic sutures generates large bending stresses, which are tensional in the flexure outer arc (i.e. atop the forebulge; Turcotte and Schubert, 1982). Whether the bending stress may be the cause for the joints observed in exposures of the Apulian and Hyblean forebulges is hereafter tested analytically.

By assuming a simple elastic model of cylindrical flexure, in which the foreland lithosphere is characterised by a constant flexural rigidity and is approximated to a



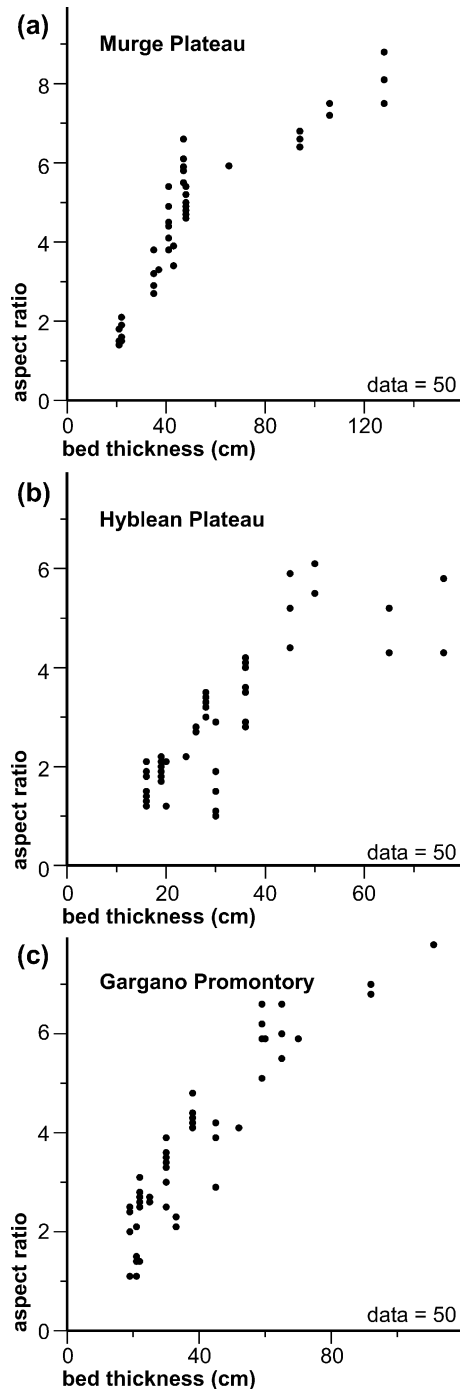


Fig. 7. Diagrams of the average aspect ratio of fracture-bound blocks (see Fig. 4a for explanations about the fracture-bound blocks) versus the relative bed thickness for (a) the Apulian Plateau, (b) the Hyblean Plateau, and (c) the Gargano Peninsula. These diagrams show an overall direct correlation between bed thickness and the aspect ratio of fracture-bound blocks regardless of the fracture type (i.e. joint or cleavage).

semi-infinite thin elastic plate subject to a linear end load, the bending stress ( $\sigma_{xx}$ , also known as fibre stress) atop the forebulge is (Turcotte and Schubert, 1982):

$$\sigma_{xx} = -6 M_b/T_e^2 \quad (1)$$

where  $M_b$  is the flexural moment in the forebulge and  $T_e$  is the effective elastic thickness of the lithosphere.  $\sigma_{xx}$  is parallel to the flexed layers and perpendicular to the flexural axis.  $M_b$  is:

$$M_b = -(\pi^2/8)[Dw_b/(x_b - x_0)^2] \quad (2)$$

where  $D$  is the flexural rigidity,  $w_b$  is the vertical upward deflection of the forebulge and  $x_b - x_0$  is the horizontal half-width of the forebulge.  $D$  is:

$$D = -(ET_e^3)/[12(1 - \nu^2)] \quad (3)$$

where  $E$  is the Young's modulus and  $\nu$  is the Poisson's ratio.

Royden (1988), Cogan et al. (1989) and Billi and Salvini (2003) developed the flexural models for the Apulian and Hyblean lithospheres and provided the appropriate flexural parameters (i.e.  $D$ ,  $T_e$ ,  $w_b$  and  $x_b - x_0$ ) to compute, through Eqs. (1)–(3), the theoretical bending stress atop the relative forebulges (Table 1). From these parameters, the bending stress atop the Apulian and Hyblean forebulges is about  $-142$  and  $-128$  MPa (i.e. negative values denote tensile stresses), respectively. These stresses are, in module, well in excess of the tensile strength that commonly characterises carbonate rocks under ambient conditions (i.e. usually between  $\sim 4$  and  $\sim 20$  MPa; e.g. Paterson, 1978). This shows that the lithosphere flexure is a suitable process for the generation of the joints observed atop the Apulian and Hyblean forebulges, in particular those joints parallel to the major flexural axes, namely the NW-trending joints in the Apulian forebulge and the NE-trending joints in the Hyblean forebulge. The large disparity between the carbonate strength and the theoretical bending stresses in the Apulian and Hyblean forebulges implies that part of the bending stress have been probably relieved by rock fracturing also in the subsurface, consistently with the strength of rocks under confining pressures. This process may explain the occurrence, in the Apulian and Hyblean regions, of important hydrocarbon deposits sourced from and accumulated in fractured foreland carbonates at depths shallower than about 5000 m (Mattavelli et al., 1993).

The above model for the cylindrical flexure of the Apulian and Hyblean forelands cannot alone explain the orthogonal sets of joints observed in these areas (Fig. 5b

Table 1

Flexural parameters for the Apulian and Hyblean flexed continental forelands (compiled after Royden (1988), Cogan et al. (1989) and Billi and Salvini (2003))

Flexural parameters	Apulia	Hyblea
$D$ (Nm)	$10^{21}$	$10^{21}$
$T_e$ (m)	11,100	8000
$w_b$ (m)	1000	1000
$x_b - x_0$ (m)	60,000	30,000
$\sigma_{xx}$ atop forebulge (MPa)	$-142$	$-128$

$D$ : flexural rigidity;  $T_e$ : effective elastic thickness;  $w_b$ : vertical upward deflection of the forebulge;  $x_b - x_0$ : horizontal half-width of the forebulge;  $\sigma_{xx}$ : bending stress (negative values when tensile).

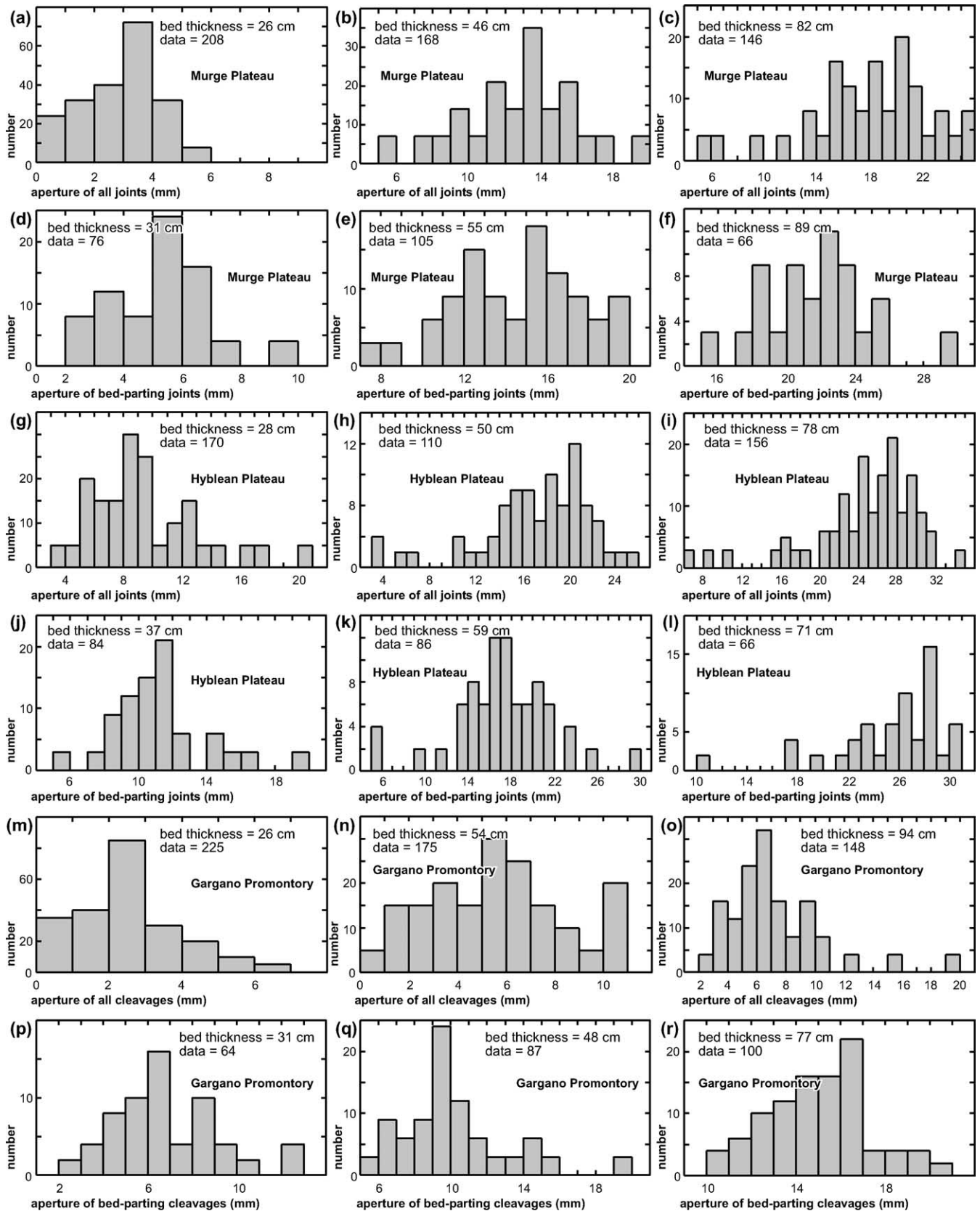


Fig. 8. Frequency histograms of aperture of joints ((a)–(l)) and cleavages ((m)–(r)) analysed along 18 selected scan-lines. (a)–(f) refer to the Apulian Plateau, (g)–(l) refer to the Hyblean Plateau, and (m)–(r) refer to the Gargano Peninsula. (a)–(c), (g)–(i) and (m)–(o) refer to fracture aperture as measured on bed cross-sections (i.e. all fractures), whereas (d)–(f), (j)–(l) and (p)–(r) refer to fracture aperture as measured over the bedding surfaces (i.e. only bed-parting fractures).



and c). The joint crosscutting relationships in the Apulian and Hyblean forebulges show that the joints parallel to the flexure axis substantially predate the orthogonal set of joints (i.e. the flexure-perpendicular joints usually abut against the orthogonal ones). It follows that the secondary set of joints (i.e. those that are perpendicular to the main flexural axis) developed after or in a late stage of the flexural process, when the carbonate beds had already been split into orthorhombic, joint-bound blocks (Fig. 5b and c) during the early jointing process (e.g. Gross, 1993). The development of the secondary set of joints can therefore be explained by the transverse fracturing of these blocks. Because of their orthorhombic symmetry, such blocks can undergo high flexural moments and, hence, large bending stresses (see Eq. (1)), depending on the length of their long axis. By assuming a linear elastic bending of the orthorhombic rock blocks, the flexural moment is (Turcotte and Schubert, 1982):

$$M = -V_a L/2 \quad (4)$$

where  $V_a$  is the applied force and  $L$  is the long axis of the orthorhombic blocks (i.e. possibly coinciding with  $S$  as shown in Fig. 4). By combining Eqs. (1) and (4), the applied force is:

$$V_a = \sigma_{xx} T_e^2 / 3L \quad (5)$$

where  $\sigma_{xx}$  is the tensile strength of the orthorhombic block and  $T_e$  is its effective elastic thickness, which approximately corresponds with the short axis of the orthorhombic block. For limestone under ambient conditions,  $\sigma_{xx}$  is, in module, between about 4 and 20 MPa. For the studied rock blocks,  $T_e$  is between about 0.1 and 3 m (i.e. corresponding to the bed thickness or to the spacing of bed-parting joints) and  $L$  is between a maximum of several meters (i.e. before transverse fracturing of rock blocks) and a minimum of about 0.5 m (i.e. after repeated transverse fracturing of rock blocks).  $V_a$  necessary to break apart (i.e. dilational mode) the orthorhombic blocks under flexure is in the  $10^2$ – $10^7$  N range, depending on the values used for the parameters of Eq. (5). This range of forces (i.e.  $10^2$ – $10^7$  N) is geologically likely and may have been reached in the study areas because of the non-cylindrical flexures of the lithospheres (Royden et al., 1987; Ben-Avraham et al., 1995; Mariotti and Doglioni, 2000), which generated high bending stresses also in the direction parallel to the main flexural axes (i.e. NW–SE for the Apulian forebulge and NE–SW for the Hyblean forebulge).

The development of fault-related solution cleavage in the Gargano strike-slip fault domain has been addressed in a previous paper (Salvini et al., 1999). Cleavage is hypothesised to have formed as a systematic array of solution surfaces during slow contractional strain ahead of the fault tip. As the fault propagated, it cut across the solution surfaces, which formed a damage zone surrounding the fault core where fault surfaces and fault rocks occurred. During

faulting, several solution surfaces were reactivated by shear and dilational displacements such that these surfaces propagated through the bedding surfaces (i.e. bed-parting cleavages). The model proposed by Salvini et al. (1999) is similar to the one by Petit and Barquins (1988), who observed, in laboratory experiments of fault growth across polymers, the formation of systematic joints ahead of the propagating fault tip. The different fracture types developed mostly because of different material properties (i.e. carbonates and polymers).

Although the Gargano Peninsula lies along the north-western prolongation of the Apulian forebulge axis (Fig. 1), in the Gargano Peninsula there is no evidence of the systematic joints (i.e. parallel and perpendicular to the flexural axis), which were observed in the Apulian forebulge. This suggests that the Gargano Peninsula did not undergo the process of lithosphere flexure, probably because, since the onset of the foreland flexure, it acted as an accommodation zone between adjacent foreland compartments characterised by differential processes of flexure (Mariotti and Doglioni, 2000).

## 5.2. Implications for fluid flow

Fig. 9 qualitatively illustrates the deformational patterns observed in the studied foreland carbonates and the relative potential fluid flow at shallow depths. Three cases are considered: (1) a forebulge domain characterised by a succession of carbonate beds affected by bed-parting and bed-unparting joints, and by rare faults (Fig. 9b); (2) a forebulge domain characterised by a succession of interleaved beds of carbonates and soft marls (Fig. 9c). The carbonate beds are affected by bed-parting and bed-unparting joints, and by rare faults, whereas the marls are affected by very rare joints; and (3) an intraforeland strike-slip fault domain characterised by a succession of carbonate beds affected by bed-parting and bed-unparting solution cleavages, and by several fault surfaces with associated fault rocks (Fig. 9d). The first case (Fig. 9b) is appropriate for the Apulian and Hyblean forebulges, the second case (Fig. 9c) is appropriate for the Hyblean forebulge (Fig. 5f) and the third case (Fig. 9d) is appropriate for the Gargano strike-slip fault domain. Data provided in this paper about the fracture attributes (Figs. 6–8) allow the estimation of the fracture-related rock porosity for the domains of Fig. 9b–d. In each domain, two cases are considered: (1) the porosity given by both bed-parting and bed-unparting fractures in horizontal cross-sections (i.e.  $X$ -,  $X'$ - and  $X''$ -cross-sections in Fig. 9b–d, respectively). This porosity is significant for the horizontal flow of fluids (i.e. in particular, the flow parallel to the main set of fractures); and (2) the porosity given only by the bed-parting fractures in vertical cross-sections (i.e.  $Y$ -,  $Y'$ - and  $Y''$ -cross-sections in Fig. 9b–d, respectively). This porosity is significant for the vertical flow of fluids; however, depending on the fracture connectedness, also the bed-unparting fractures may partly contribute to the vertical

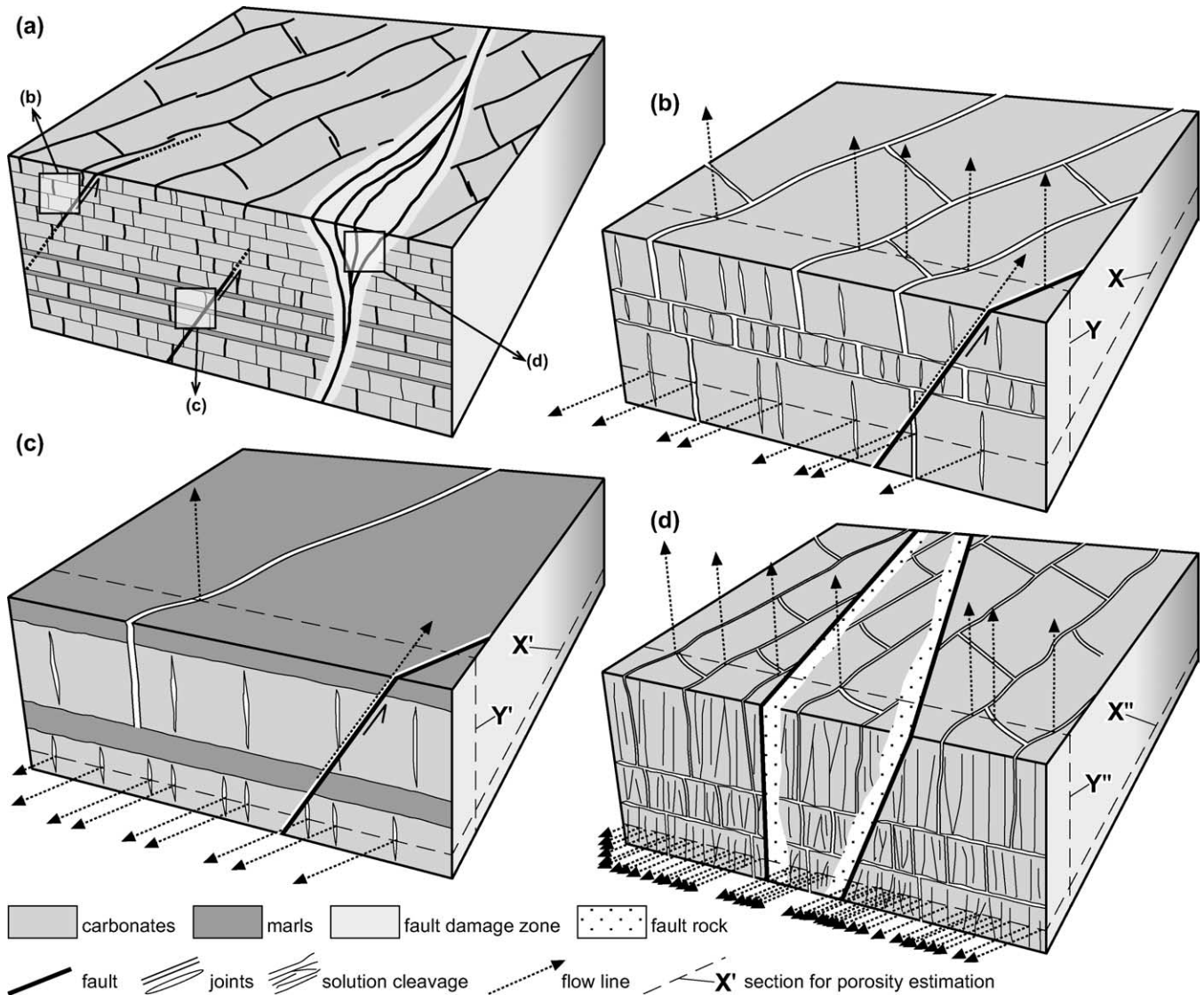


Fig. 9. Conceptual model of fluid flow through foreland carbonate beds. The model is based on the data provided in Figs. 6–8 about the fracture attributes. (a) Overview. (b)–(d) Specific cases suitable for the study areas.

flow of fluids. In the porosity estimations, the contribution of the void occurring along the bedding surfaces is not considered. Each estimation applies to a single bed with a given thickness (i.e. ~50 cm). The following estimations of porosity should be considered as upper-bound values because of possible inaccuracies in the measure of fracture apertures in rock exposures; however, regardless of the porosity real values, the disparities between porosities estimated in horizontal and vertical cross-sections are significant to infer potential anisotropies of fluid flow.

By considering a ~50-cm-thick carbonate bed containing joints (both bed-unparting and bed-parting) with an average spacing of 10 cm (Fig. 6a and c) and an average aperture of 1 cm (Fig. 8b), the porosity in the X-cross-section of Fig. 9b is about 11%. In contrast, by considering data about the bed-parting fractures in the same ideal bed (joint spacing from Figs. 6b and d and 7a and b; joint

aperture from Fig. 8e and k) the porosity in the Y-cross-section of Fig. 9(b) is about 5%.

The porosity of beds illustrated in Fig. 9c is similar to that of beds in Fig. 9b; however, in Fig. 9c, the occurrence of almost unfractured layers of soft marls (e.g. Fig. 5f) may hinder the vertical flow of fluids. Vertical flows may, in fact, solely occur along paths generated by occasional joints across marls and by occasional high-angle faults (Fig. 9c).

By considering a ~50-cm-thick carbonate bed containing fault-related solution cleavage (both bed-unparting and bed-parting) with an average spacing of 7.5 cm (Fig. 6e) and an average aperture of 0.5 cm (Fig. 8n), the porosity in the X''-section of Fig. 9d is about 7%. In contrast, by considering data about the bed-parting cleavage in the same ideal bed (cleavage spacing from Figs. 6f and 7c; cleavage aperture from Fig. 8q) the porosity in the Y''-cross-section of Fig. 9d is about 2.5%. In such a tectonic domain, however,



the rock porosity may significantly increase because of intense fracturing, which usually occurs in the portion of the damage zone near the fault core (e.g. Billi et al., 2003). In contrast, the porosity and permeability of fault rocks depend mostly on the particle size distribution and packing (e.g. Antonellini and Aydin, 1994; Caine et al., 1996).

## 6. Conclusions

From the analysis of three foreland areas of southern Italy, the following main conclusions can be drawn:

- (1) Near-horizontal carbonate beds from apparently slightly deformed forelands can be intensely fractured by regional tectonic processes such as the lithosphere flexure near orogenic sutures or the development of intraforeland strike-slip fault belts. Intense deformational fabrics of rocks can therefore occur before foreland rocks are incorporated in fold–thrust belts.
- (2) Regardless of the different tectonic histories, the studied foreland rocks are affected by similar fracture networks consisting in orthogonal sets of sub-vertical, tectonic discontinuities, which transformed the pristinely continuous carbonate beds into an assemblage of orthorhombic, fracture-bound blocks.
- (3) From the distribution and attributes of fractures in the studied foreland rocks, a poor-to-fair fracture-related porosity (<15%) is estimated and a markedly anisotropic permeability is inferred.

## Acknowledgements

I thank P. Gillespie, R. Jolly, T. Needham and D. Peacock for insightful reviews, R. Funicello, M. Mattei, C. Monaco, C. Poloni, M. Porreca, F. Storti, S. Tavani, M. Tiberti, L. Tortorici and G. Vignaroli for their help and suggestions. Fieldwork was carried out under the supervision of F. Salvini (Apulian foreland) and C. Faccenna (Hyblean foreland). Fieldwork was partly supported by a GNDT Project coordinated by L. Beranzoli with the help of P. Favali. Schmidt diagrams were elaborated with the Daisy 3 software kindly provided by F. Salvini.

## References

- Antonellini, M., Aydin, A., 1994. Effect of faulting on fluid flow in porous sandstones: petrophysical properties. *American Association of Petroleum Geologists Bulletin* 78, 355–377.
- Aydin, A., 2000. Fractures, faults, and hydrocarbon entrapment, migration, and flow. *Marine and Petroleum Geology* 17, 797–814.
- Bai, T., Pollard, D.D., Gao, H., 2000. Explanation for fracture spacing in layered materials. *Nature* 403, 753–756.
- Barrier, E., 1992. Tectonic analysis of a flexed foreland: the Ragusa Platform. *Tectonophysics* 206, 91–111.
- Ben-Avraham, Z., Lyakhovskiy, V., Grasso, M., 1995. Simulation of collision zone segmentation in the central Mediterranean. *Tectonophysics* 243, 57–68.
- Bertotti, G., Picotti, V., Chilovi, C., Fantoni, R., Merlini, S., Mosconi, A., 2001. Neogene to Quaternary sedimentary basins in the south Adriatic (Central Mediterranean): foredeeps and lithospheric buckling. *Tectonics* 20, 771–787.
- Billi, A., Salvini, F., 2003. Development of systematic joints in response to flexure-related fibre stress in flexed foreland plates: the Apulian forebulge case history, Italy. *Journal of Geodynamics* 36, 523–536.
- Billi, A., Storti, F., 2004. Fractal distribution of particle size in carbonate cataclastic rocks from the core of a regional strike-slip fault zone. *Tectonophysics* 384, 115–128.
- Billi, A., Salvini, F., Storti, F., 2003. The damage zone–fault core transition in carbonate rocks: implications for fault growth, structure and permeability. *Journal of Structural Geology* 25, 1779–1794.
- Blenkinsop, T.G., Vearncombe, J.R., Reddy, S.M. (Eds.), 2004. Applied structural geology for mineral exploration and mining *Journal of Structural Geology*, 26, pp. 6–7.
- Brankman, C., Aydin, A., 2004. Uplift and contractional deformation along a segmented strike-slip fault system: the Gargano Promontory, southern Italy. *Journal of Structural Geology* 26, 807–824.
- Brusseau, M.L., 1994. Transport of reactive contaminants in heterogeneous porous media. *Reviews of Geophysics* 32, 285–313.
- Caine, J.S., Tomasiak, S.R.A., 2003. Brittle structures and their role in controlling porosity and permeability in a complex Precambrian crystalline-rock aquifer system in the Colorado Rocky Mountain Front Range. *Geological Society of America Bulletin* 115, 1410–1424.
- Caine, J.S., Evans, J.P., Forster, C.B., 1996. Fault zone architecture and permeability structure. *Geology* 24, 1025–1028.
- Clauser, C., 1992. Permeability of crystalline rocks. *Eos* 73, 237–238.
- Cogan, J., Rigo, L., Grasso, M., Lerche, I., 1989. Flexural tectonics of southeastern Sicily. *Journal of Geodynamics* 11, 189–241.
- Darcel, C., Davy, P., Bour, O., 2004. Influence of spatial correlation of fracture centers on the permeability of two-dimensional fracture networks following a power law length distribution. *Water Resources Research* 40, W01502. doi:10.1029/2003WR002260.
- D'Argenio, B., 1974. Le piattaforme carbonatiche periadriatiche. Una rassegna di problemi nel quadro geodinamico mesozoico dell'area mediterranea. *Memorie della Società Geologica Italiana* 13, 137–159.
- Dewey, J.F., Helman, M.L., Turco, E., Hutton, D.H.W., Knott, S.D., 1989. Kinematics of the western Mediterranean. In: Coward, M.P., Dietrich, D., Park, R.G. (Eds.), *Alpine Tectonics Special Publication*, vol. 45. Geological Society, London.
- Dholakia, S.K., Aydin, A., Pollard, D.D., Zoback, M.D., 1998. Fault-controlled hydrocarbon pathways in the Monterey Formation, CA. *American Association of Petroleum Geologists Bulletin* 82, 1551–1574.
- Dogliani, C., Mongelli, F., Pieri, P., 1994. The Puglia uplift (SE Italy): an anomaly in the foreland of the Apenninic subduction due to buckling of a thick continental lithosphere. *Tectonics* 13, 1309–1321.
- de Dreuzy, J.-R., Davy, P., Bour, O., 2001. Hydraulic properties of two-dimensional random fracture networks following power law length distribution 2. Permeability of networks based on lognormal distribution of apertures. *Water Resources Research* 37, 2079–2095.
- Eichub, P., Taylor, W.L., Pollard, D.D., Aydin, A., 2004. Palaeo-fluid flow deformation in the Aztec Sandstone at the Valley of Fire, Nevada—evidence for the coupling of hydrogeologic, diagenetic, and tectonic processes. *Geological Society of America Bulletin* 116, 1120–1136.
- Engelder, T., Scholz, C., 1981. Fluid flow along very smooth joints at effective pressure up to 200 megapascals. In: Carter, N.L. (Ed.), *Mechanical behavior of crustal rocks Geophysical Monograph Series*, vol. 24. AGU, pp. 147–152.
- Favali, P., Funicello, R., Mattiotti, G., Mele, G., Salvini, F., 1993. An active margin across the Adriatic Sea (central Mediterranean Sea). *Tectonophysics* 219, 109–117.

- Fletcher, R.C., Pollard, D.D., 1981. Anticrack model for pressure solution surfaces. *Geology* 9, 419–424.
- Gerritsen, M.G., Durllofsky, L.J., 2005. Modeling fluid flow in oil reservoirs. *Annual Review of Fluid Mechanics* 37, 211–238.
- Gillespie, P.A., Johnston, J.D., Loriga, M.A., McCaffrey, K.L.W., Walsh, J.J., Watterson, J., 1999. Influence of layering on vein systematics in line samples. In: McCaffrey, K.L.W., Lonergan, L., Wilkinson, J.J. (Eds.), *Fractures, Fluid Flow and Mineralisation Special Publication*, vol. 155. Geological Society, London, pp. 35–56.
- Grasso, M., Pedley, H.M., 1990. Neogene and Quaternary sedimentation patterns in the northwest Hyblean Plateau (SE Sicily): the effect of a collisional process on a foreland margin. *Rivista Italiana di Paleontologia e Stratigrafia* 96, 219–240.
- Gross, M.R., 1993. The origin and spacing of cross joints: examples from the Monterey Formation, Santa Barbara Coastline, California. *Journal of Structural Geology* 15, 737–751.
- Gudmundsson, A., 2000. Fracture dimensions, displacements and fluid transport. *Journal of Structural Geology* 22, 1221–1231.
- Kulander, B.R., Dean, S.L., 1985. Hackle plume geometry and joint propagation dynamics. In: Stephansson, O. (Ed.), *Fundamentals of Rock Joints*. Centek Publishers, Lulea, Sweden, pp. 85–94.
- Malinverno, A., Ryan, W.B.F., 1986. Extension in the Tyrrhenian Sea and shortening in the Apennines as result of arc migration driven by sinking of the lithosphere. *Tectonics* 5, 227–254.
- Mariotti, G., Doglioni, C., 2000. The dip of the foreland monocline in the Alps and Apennines. *Earth and Planetary Science Letters* 181, 191–202.
- Mattavelli, L., Pieri, M., Groppi, G., 1993. Petroleum exploration in Italy: a review. *Marine and Petroleum Geology* 10, 410–425.
- Narr, W., Currie, J.B., 1982. Origin of fracture porosity—example from Altamont Field, Utah. *American Association of Petroleum Geologists Bulletin* 66, 1231–1247.
- Nelson, R.A., 2001. *Geologic Analysis of Naturally Fractured Reservoirs*, 2nd edition Gulf Professional Publishing, Houston.
- Neretnieks, I., 1985. Transport in fractured rocks. *International Contributions to Hydrogeology Memoirs* 17, 301–318.
- Neuman, S.P., Di Federico, V., 2003. Multifaceted nature of hydrogeologic scaling and its interpretation. *Reviews of Geophysics* 41, 1014. doi:10.1029/2003RG000130.
- Odling, N.E., Gillespie, P.A., Bourguine, B., Castaing, C., Chiles, J.P., Christensen, N.P., Fillion, E., Genter, A., Olsen, C., Thrane, L., Trice, R., Aarseth, E., Walsh, J., Watterson, J.J., 1999. Variations in fracture system geometry and their implications for fluid flow in fractured hydrocarbon reservoirs. *Petroleum Geosciences* 5, 373–384.
- Patacca, E., Scandone, P., 2001. Late thrust propagation and sedimentary response in the thrust-belt-foredeep system of the Southern Apennines (Pliocene–Pleistocene). In: Vai, G.B., Martini, I.P. (Eds.), *Anatomy of an Orogen: the Apennines and Adjacent Mediterranean Basins*. Kluwer Academic Publishers, London, pp. 401–440.
- Paterson, M.S., 1978. *Experimental Rock Deformation: the Brittle Field*. Springer, Berlin.
- Petit, J.-P., Barquins, M., 1988. Can natural faults form under Mode II conditions? *Tectonics* 7, 1243–1256.
- Pollard, D.D., Aydin, A., 1988. Progress in understanding jointing over the past century. *Geological Society of America Bulletin* 100, 1181–1204.
- Price, N.J., 1966. *Fault and Joint Development in Brittle and Semi-brittle Rocks*. Pergamon Press, Oxford.
- Royden, L., 1988. Flexural behavior of the continental lithosphere in Italy: constraints imposed by gravity and deflection data. *Journal of Geophysical Research* 93, 7747–7766.
- Royden, L., Patacca, E., Scandone, P., 1987. Segmentation and configuration of subducted lithosphere in Italy: an important control on thrust-belt and foredeep-basin evolution. *Geology* 15, 714–717.
- Salvini, F., Billi, A., Wise, D.U., 1999. Strike-slip fault-propagation cleavage in carbonate rocks: the Mattinata Fault zone. *Journal of Structural Geology* 21, 1731–1749.
- Sibson, R.H., 1996. Structural permeability of fluid-driven fault-fracture meshes. *Journal of Structural Geology* 18, 1031–1042.
- Taylor, W.L., Pollard, D.D., Aydin, A., 1999. Fluid flow in discrete joint sets: field observations and numerical simulations. *Journal of Geophysical Research* 104, 28983–29006.
- Turcotte, D.L., Schubert, G., 1982. *Geodynamics*. Wiley, New York.
- Yellin-Dror, A., Grasso, M., Ben-Avraham, Z., Tibor, G., 1997. The subsidence history of the northern Hyblean plateau margin, southeastern Sicily. *Tectonophysics* 282, 277–289.
- Zarudski, E.F.K., 1972. The strait of Sicily—a geophysical study. *Revue de Géographie Physique et de Géologie Dynamique* 14, 11–28.